Domain relaxation dynamics in epitaxial BiFeO3 films: Role of surface charges

Yi-Chun Chen, Cheng-Hung Ko, Yen-Chin Huang, Jan-Chi Yang, and Ying-Hao Chu

Citation: Journal of Applied Physics **112**, 052017 (2012); doi: 10.1063/1.4746077
View online: http://dx.doi.org/10.1063/1.4746077
View Table of Contents: http://scitation.aip.org/content/aip/journal/jap/112/5?ver=pdfcov
Published by the AIP Publishing

Domain relaxation dynamics in epitaxial $BiFeO_3$ films: Role of surface charges

Yi-Chun Chen (陳宜君),[1] Cheng-Hung Ko (柯政宏),[1] Yen-Chin Huang (黃彥欽),[1] Jan-Chi Yang (楊展其),[2] and Ying-Hao Chu (朱英豪)[2]
[1]*Department of Physics, National Cheng Kung University, Tainan 70101, Taiwan*
[2]*Department of Materials Science and Engineering, National Chiao Tung University, Hsinchu 30010, Taiwan*

(Received 16 December 2011; accepted 29 May 2012; published online 4 September 2012)

The thermodynamic parameters of domain relaxation process in the absence of external electric fields are related to the intrinsic electrostatic and stress/strain conditions inside the materials, such as the states at surface, states at interface with the electrode, and the atomic defects in the bulk. In order to perform systematical studies of these intrinsic effects, we investigated domain relaxation in a monodomain environment, which was obtained in strained epitaxial $BiFeO_3$ (BFO)(111) films. Without as-grown domain walls and grain boundaries, the epitaxial BFO (111) film provided an ideal system for the dynamic observation of 180-degree domain wall motion. Nano-domains were initially created by writing voltage pulses under the tip of a scanning force microscope and then relaxed through time. The downward polarized domains exhibited much better retention behaviors than the upward domains. A two-step backswitching process was observed, and the behaviors varied with the initial domain sizes. Surface potential measurement showed the dissipation of surface screen charges with time, which was strongly coupled with the 1st step relaxation. The asymmetry behaviors for upward and downward backswitchings, and the two-stage relaxation processes can be explained by the mobile vacancies and the redistribution of surface charges. This study provides the basic understanding of the role of surface charges during the ferroelectric domain relaxation. © *2012 American Institute of Physics*. [http://dx.doi.org/10.1063/1.4746077]

I. INTRODUCTION

The retention behavior of ferroelectric domains provides desirable ability for application to electronic nonvolatile memories and functional devices.[1,2] The ferroelectric polarization switching dynamics, which involves domain nucleation and growth, was the key issue in many aspects, including domain stability, manipulation, response speeds and size limits, and so had been widely investigated.[3–24] The most useful tool to examine the domain wall kinetics at nanoscale is the high-resolution piezoresponse force microscope (PFM). When external bias was applied through the tip, the polarization switching process started from a single nucleation below the tip, which was then followed by domain growth. Observation of the series of domain wall motion and intermediate stable domain structures can provide detailed thermodynamic information of domain switching.[8–18] In contrast to the field-driven nucleation studies, where the external field energy is the dominant factor, investigation of domain relaxation with time in the absence of electric fields shows more intrinsic response from the material system. The depolarization field resulting from the incomplete compensation of polarization bound charges at boundaries was suggested as the main mechanism of ferroelectric retention failure.[25] Dynamics of domain relaxation will therefore reflect the evolution of space charge distribution at the surface of the film or the interface between the film and electrode. Until now, the domain backswitching at nanoscale was only addressed in few cases,[19–24] which showed the relaxation behaviors were coupled with complicated local environmental parameters, such as different types of domain wall, polycrystalline orientation, and grain boundaries.

Recent studies had shown successful conduction modulation in ferroelectric films by changing spontaneous polarization directions.[26–29] The concept of this phenomenon was mainly based on the space charge redistribution in the ferroelectric tunneling junction or the depletion layer at the interface. Latest advances in scanning probe microscope (SPM) technique had achieved a high-resolution specification to image surface charges on a length scale down to 25 nm.[30] Revealing the key factors to control surface electrostatics in ferroelectrics, such as screen and polarization bound charges,[31–33] will be an important step for advanced electronic devices. On the other hand, the electric-field-controllable conductive states will also affect the retention behaviors of ferroelectric domains. In this study, in order to systematically investigate the domain relaxation dynamics under the influence of surface or interface charges, we chose the multiferroic $BiFeO_3$ (BFO) epitaxial film grown on the (111) $SrTiO_3$ (STO) substrate as the tested sample, which resembles an ideal monodomain environment.[34] Without as-grown domain walls or grain boundaries, the key factors to determine the backswitching domain dynamics will be the surface states, interface states, or intrinsic atomic defects in films, such as vacancies. The role of surface charge distribution was further investigated by using Kelvin probe force microscope (KFM, i.e., surface potential microscope).

II. EXPERIMENT

The BFO(111) films of 100 nm thickness were epitaxially grown on the $SrRuO_3$ (SRO) buffered STO(111) single crystal substrates by pulsed laser deposition (PLD) method. The conductive SRO layer was served as the bottom electrode for electrical testing. BFO is one of the few room-temperature single-phase multiferroics, with relatively high ferroelectric Curie temperature ($T_c \sim 1100$ K) and antiferromagnetic Néel temperature ($T_N \sim 640$ K).[35] The crystal structure of BFO is a rhombohedrally distorted perovskite ($a_r = 3.965$ Å and $\alpha_r = 0.6°$), which has eight low-energy ferroelectric variants along one the four pseudo-cubic diagonals ⟨111⟩ directions.[36] For epitaxial BFO(111)/STO(111) films, the in-plane compressive stress from the substrate breaks the symmetry of eight polarization variants, leaving two lowest energy states, out-of-plane downward and upward polarizations.[34] Epitaxial growth of the BFO(111) films was confirmed by x-ray diffraction, and the as-grown domain structures were tested by PFM. A commercial scanning probe microscope (CPII, Veeco) equipped with a lock-in amplifier (SR-830, Stanford Research Systems) was used to perform PFM measurements. The voltage pulses to create domains were applied from an arbitrary waveform generator (G5100A, PICOTEST), which was directly connected to the tip and switched off during PFM imaging. The scanning tip was a commercial Pt-Ir coated tip with elastic constants about 7 N/m (PPP-NCSTPt-20, Nanosensors), and the modulation ac voltage for PFM domain imaging was 1.0 V at 6.39 kHz. KFM was operated in tapping mode with dc voltage feedback turned on for surface potential imaging, and its modulation ac voltage was 1.0 V at 20 kHz.

III. RESULTS AND DISCUSSION

PFM images in Figure 1 show the relaxation evolution of BFO domains created by pulse voltages. There are only two contrasts in each image, where the bright and dark contrasts correspond to the upward and downward polarized domains, respectively. Note that although these two polarization variants perpendicular to the film surface are of relatively low energy, the self-poling effect from SRO bottom electrodes causes the as-grown film a single domain environment with only downward polarization. The upward polarized nano-domains in Fig. 1 were switched by applying voltage pulses directly on the as-grown downward polarized matrix. In contrast, to study downward polarized nano-domains, an upward polarized area needed to be pre-switched as the single-domain environment for nucleation. In our previous studies,[13] the sizes of both downward and upward polarized domains can be controlled by writing pulse duration and voltage magnitudes, with the average standard deviations smaller than 5%. The domains in Fig. 1 were all switched by voltage pulses with magnitude of 10 V. Under this voltage, the domain radius increased quickly with the writing time and then approached to an equilibrium size with diameter about 120 nm. After that, an abrupt increase of domain size only occurred under longer switching voltage pulses ($>10^5$ μs),[13] which had also been observed in other studies,[18] but the possible explanation was still unclear. By studying the relaxation behaviors of thus

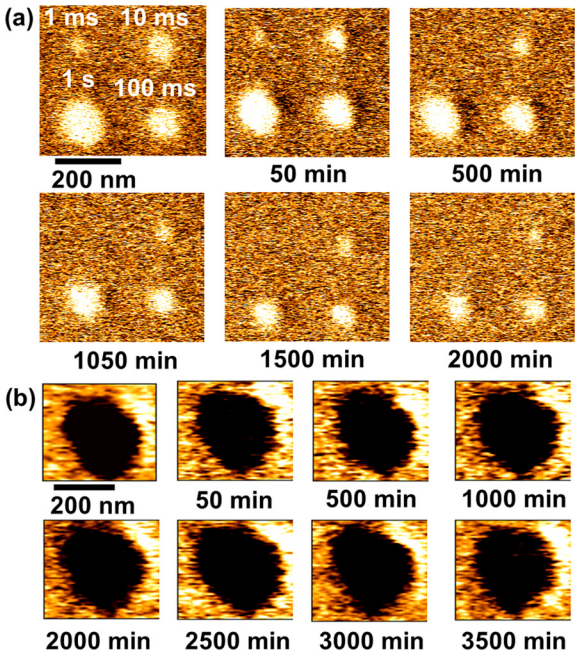

FIG. 1. Typical domain evolution with time after the switching field is removed. (a) PFM images of upward polarized ferroelectric domains just switched and measured after 50 min, 500 min, 1050 min, 1500 min, and 2000 min. The domains were written by −10 V tip bias with pulse duration of 1 ms, 10 ms, 100 ms, and 1 s. (b) PFM images of downward polarized ferroelectric domains just switched and measured after 50 min, 500 min, 1000 min, 2000 min, 2500 min, 3000 min, and 3500 min. The domains were written by +10 V tip bias with duration of 1 s.

formed domains, the phenomenon of abnormal domain regrowth can be attributed to the charge redistribution during poling process and will be discussed later. Fig. 1 shows the upward polarized nano-domains backswitched to smaller sizes, while the downward polarized domains slightly increased with time, i.e., both tended to relax to the as-grown polarizations. Our previous study also showed the activation energy for the growth of downward polarized domains is lower than that of the upward polarized domains.[13]

Figures 2(a) and 2(b) show the systematical testing results of the domain diameter relaxed with time for upward and downward polarized domains, respectively. Domains with different initial sizes were all written by voltage with magnitude of 10 V but different pulse duration time. In order to perform a quantitative analysis, all the domain sizes are converted to the fraction of retained area (F_{ret}), which is defined as 1 minus the ratio of the backswitched area to the initial domain size, and its evolution with time is shown in Fig. 2(c). All data points in Figs. 2(a) and 2(b) are analyzed and plotted in Fig. 2(c), and it is interesting to notice that some relaxation processes are coincided, resulting in three groups of normalized relaxation trends, i.e., (i) upward polarized domains with initial diameter $d_0 > 170$ nm (red open symbols), (ii) upward polarized domains with initial diameter $d_0 < 170$ nm (blue solid symbols), and (iii) downward polarized domains (gray half-filled symbols). The downward polarized domains show much better retention behaviors than the upward polarized domains. Note that initial diameters larger than 170 nm were all written by longer switching voltage pulses ($>10^5$ μs), and therefore was in the abrupt

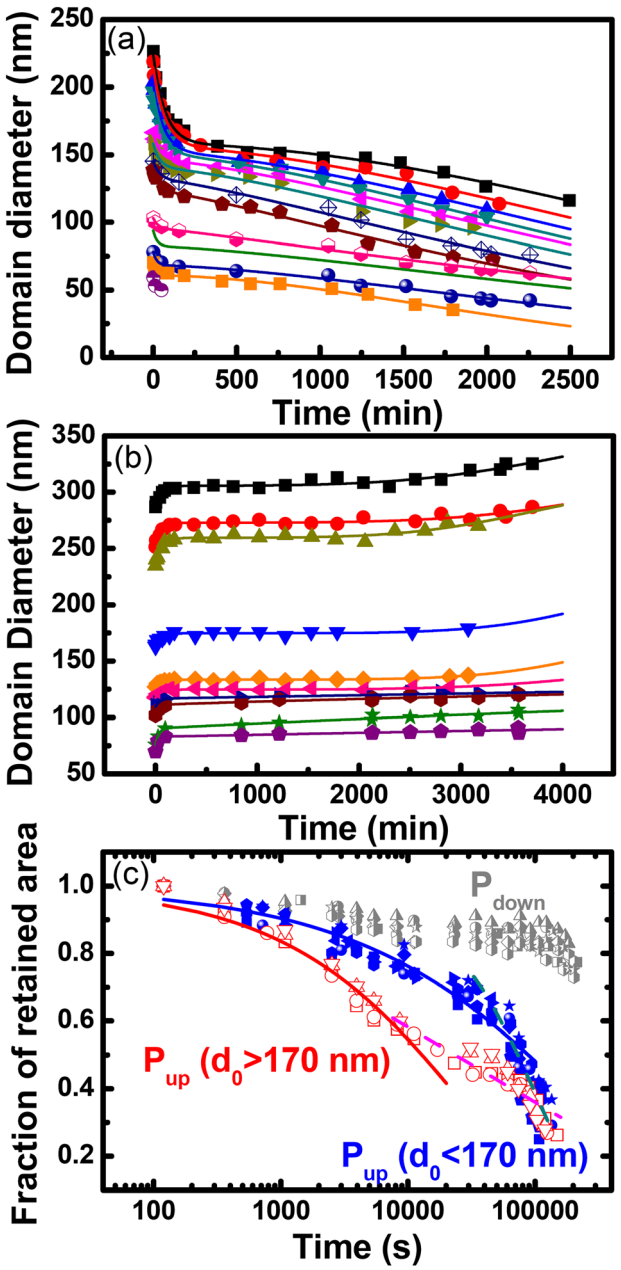

FIG. 2. Domain diameters versus the relaxation time for (a) upward and (b) downward polarized domains. Different sizes of domains were created by pulse voltages with magnitude of 10 V but different writing time. (c)Fraction of retained area versus the relaxation time analyzed from (a) and (b). The relaxation process shows three different kinds of trends corresponding to upward polarized domains with initial diameter $d_0 > 170$ nm (red open symbols), upward polarized domains with initial diameter $d_0 < 170$ nm (blue solid symbols), and downward polarized domains (gray half-filed symbols).

domain re-growth phase during the domain creation. As shown in Fig. 2(c), all relaxation dynamics of upward polarized domains need to be fitted by two stages: the 1st stage is the earlier relaxation, which follows the stretched exponential retention behavior, and the 2nd stage is the latter relaxation, which can be roughly fitted by logarithmic time dependence. The stretched exponential form corresponds to the relaxation in disorder or strongly interacting materials[37]

$$F_{\text{ret}} = \exp[-(t/\tau)^{\beta}], \quad 0 < \beta < 1, \tag{1}$$

where τ is the characteristic time for backswitching and β is the stretched exponent. The deviation of β from 1 suggested that there was a statistical distribution of characteristic relaxation time. For initial domain sizes >170 nm, the fitted $\tau = 2.57 \times 10^4$ s and $\beta = 0.53$, while for initial domain sizes <170 nm, the fitted $\tau = 2.07 \times 10^5$ s and $\beta = 0.43$. The fitted results show that domains written under longer pulses relaxed fast in the 1st stage, but when compared in a long time scale, they had better retention behaviors in the 2nd stage. The causes of two-stage relaxation and the difference between three relaxation groups will be discussed in details later.

Relaxation towards the as-grown downward polarized states can be explained by the Schottky contact at the BFO/SRO interface. The work function of SRO is 5.2 eV,[38] and the electron affinity of BFO is 3.3 eV.[39] From Schottky-Mott model,[40] if the density of interface states is extremely low, the BFO/SRO interface will be an n-type Schottky contact, with barrier height $\phi_{SB} = 1.9$ eV. Figure 3 illustrates the band diagram and the corresponding space charge distribution at the BFO/SRO interface. Due to the contribution of space charges in the depletion layers, a built-in electric field toward the SRO electrode is established on the BFO side, which reduces the activation energy for the nucleation of downward polarized domains. This built-in field breaks the equivalence of two polarization states in as-grown film, and provides a strong tendency of relaxation for all domains to downward polarization. In previous studies, it had also been suggested that the retention failures were strongly eliminated when ohmic contact electrodes were used.[20]

The difference of decaying rates between upward and downward polarized domains suggests an asymmetric distribution of depolarization fields. In Fig. 4(a), KFM image shows negative surface potential on the upward polarized domains. The polarity of surface potential is opposite to that

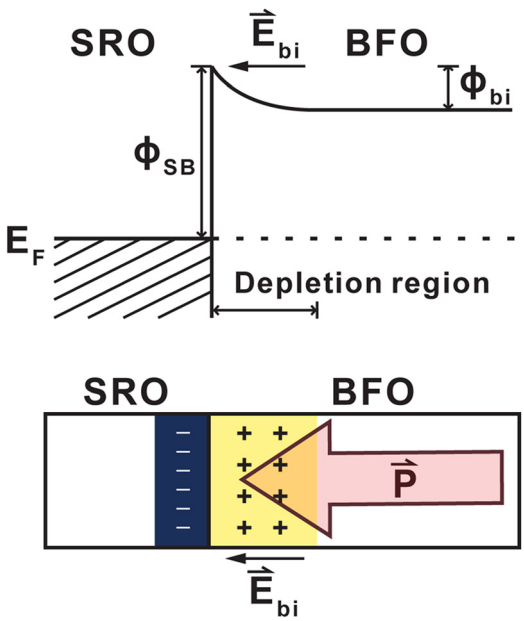

FIG. 3. Illustration of Schottky contact and space charge distribution at BFO/SRO interface. A built-in electric field toward SRO existed in the depletion region of the BFO film.

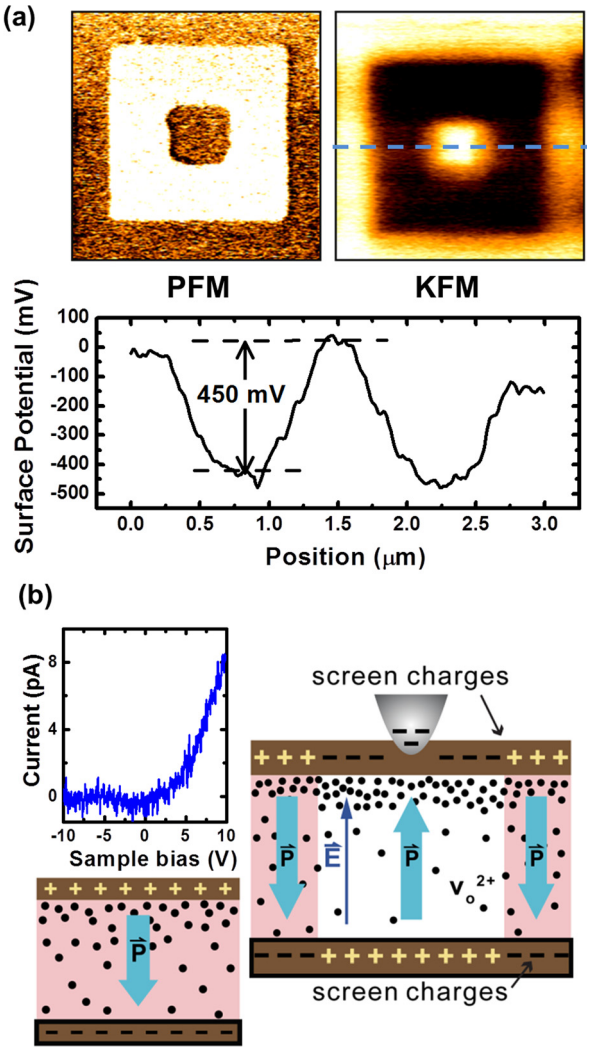

FIG. 4. (a) PFM and KFM images of switched squares. The variation of surface potential along the dash line was shown in the bottom plot. In PFM, the bright and dark contrasts correspond to upward and downward polarizations, respectively. In KFM, the bright and dark contrasts correspond to positive and negative surface potentials, respectively. (b) The diode-like I-V curve of the BFO films measured by CAFM. The bottom and right diagrams illustrated the surface charge and oxygen vacancy (V_O^{2+}) distribution for as-grown and upward switched domains, respectively.

of the ferroelectric bound charges, which also had been found in other ferroelectrics.[32] Therefore, the surface potential is considered mainly due to the screen charges on the relatively conducting surface or surface absorbate, such as water molecules. Table I shows that the surface potential contrast difference between upward and downward domains is proportional to the macroscopic saturation polarizations of different samples, and suggests that the surface potential contrast provides the information of surface screening charges. Interestingly, Table I also shows that the difference of activation fields between upward and downward domain nucleation is proportional to both the surface potential contrast and the saturation polarization. This phenomenon indicates that the depolarization field is the key factor for domain wall motion dynamics. The asymmetry of retention behaviors for upward and downward polarized domains is related to the screen charge redistribution and can be explained by the mobile vacancies in BFO. In Fig. 4(b), the

TABLE I. Comparison of the surface potentials (ΔV), macroscopic saturated polarizations (P_s), and activation fields ($\Delta\alpha$) for domain nucleation in epitaxial BFO(111) and BFO(100) films grown on SRO buffered STO substrates.

	ΔV (mV)[a]	P_s (μC/cm^2)	$\Delta\alpha$ (MV/cm)[b]
(a) BFO(111)	450	90	2.68
(b) BFO(100)	340	65	3.71
(a)/(b)	1.32	1.38	1/1.38

[a]Surface potential difference between downward and upward polarized domains.
[b]Activation field difference between downward and upward domain nucleation. The data were obtained by studies of field-driven domain growth dynamics.[14]

current-voltage (*I-V*) characteristic curves of BFO measured by conductive atomic force microscope (CAFM) shows a diode behavior. Note that the Pt coated tip also possesses a positive n-type Schottky contact with the BFO films, which is similar to the SRO electrode, so the unipolar *I-V* behavior is not determined by the metal-ferroelectric semiconductor Schottky barriers. The most possible explanation is the model of mobile oxygen vacancies proposed in the previous study of Ca-doped BFO films.[23] For undoped BFO(111) films, the carrier density is much less than the Ca-doped BFO film, so our measured CAFM current is three order smaller; however, the unipolar *I-V* characteristic is similar.

Fig. 4(b) illustrates the possible model of vacancy motion and the screen charge reaction when a voltage pulse is applied to switch the polarization from downward to upward directions. In the as-grown states, the oxygen vacancies with positive charges neutralize space charges in the film. Under external electric fields directing upward, oxygen vacancies move toward the surface and result in a more conductive donor type region near the surface. The diode-like *I-V* behavior is caused by the barrier built between the surface p-type and bottom n-type regions. In contrast, downward electric fields only redistribute the oxygen vacancies to the neutralized grown state. This asymmetric motion of vacancies causes the asymmetric *I-V* characteristics and polarization-dependent domain retention behaviors. During the upward polarized domain nucleation, the negative screen charges can transfer from the tip to the surface. For a long-pulse switching, the surface becomes more conductive and the spreading of screen charges is more effective. The abrupt growth stage of domain switching under long time pulses is because that screen charges significantly lower the depolarization fields for domain nucleation. The pulse duration time for abrupt domain growth ($>10^5$ μs) also satisfies the characteristic time for motion of oxygen vacancies.

The role of surface screen charges during relaxation process was investigated by the evolution of surface potential with time. In Fig. 5, the upward poled squares were written by tip moving rate of 1 Hz and possessed similar surface conditions as domains written by long time pulses. The surface potential of these squares decays exponentially with time, and the characteristic time of relaxation is in the order of 10^4 s, which satisfies the characteristic time of domain

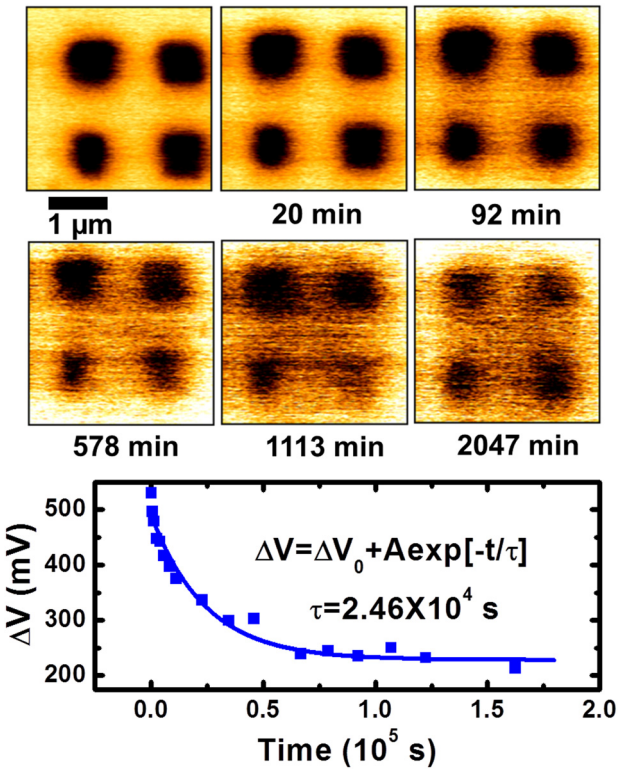

FIG. 5. KFM images of upward polarized squares just switched and measured after 20 min, 92 min, 578 min, 1113 min, and 2047 min. The squares were written by −10 V tip bias with tip scanning rate of 1 Hz. The bottom plot shows the surface potential decayed exponentially with a characteristic time of 2.46×10^4 s.

backswitching in the earlier stage. This result suggests that the dissipation of surface screen charges dominate the 1st stage of domain relaxation dynamics. Moreover, the dissipation of screen charges changes the effects to eliminate depolarization fields, and causes a time-dependent relaxation time, i.e., series-type of broad relaxation time, which leads to a stretched exponent $\beta < 1$. The phenomenon that the domains created by long pulses relax faster than those created by short pulses in the 1st relaxation stage can also be explained by the higher dissipation of screen charges in more conductive surface. After the 1st relaxation stage, the surface charges reach an equilibrium density in the absence of electric fields, and then the depolarization fields mainly depend on the geometrical factors. Since the domain wall speed followed the formula of the activated motion,[41]

$$v = \frac{dr}{dt} \sim \exp\left[-\frac{\alpha}{E_d}\right], \tag{2}$$

the depolarization field E_d as a function of domain radius r will result in a logarithmic dependence of domain sizes on time, which explains the 2nd stage of domain relaxation process. It should be noted that domains created by long pulses had better retention behaviors than those created by short pulses in the 2nd relaxation stage. This phenomenon indicated that the transfer of screening charges from the tip to BFO under long time pulses can further modify the space charge distribution in the BFO films, and cause a better equilibrium states for long time retention.

IV. CONCLUSION

The surface, interface, and vacancy effects on the domain relaxation dynamics were systematically revealed in the mono-domain-like epitaxial BFO(111) film. The built-in potential at the BFO/SRO interface will tend to relax the whole system toward downward polarizations. The asymmetric retention behaviors for upward and downward domains can be explained by the directional mobile vacancies. The KFM results show the relaxation of surface screen charges with time, which is also suggested as the dominant mechanism governing the domain relaxation in the short-time stage. The domain relaxation in the long-time stage is related to the surface conductivity and the redistribution of space charges near surface, which can be modified during the domain creation.

ACKNOWLEDGMENTS

Financial support of the National Science Council through projects NSC 99-2112-M-006-012-MY3 and NSC 100-2119-M-009-003 are gratefully acknowledged by the authors.

[1]J. F. Scott and C. A. Araujo, Science **246**, 1400 (1989).
[2]R. Waser and A. Rüdiger, Nat. Mater. **3**, 81 (2004).
[3]Y. H. Shin, I. Grinberg, I. W. Chen, and A. M. Rappe, Nature **449**, 881 (2007).
[4]M. Molotskii, J. Appl. Phys. **93**, 6234 (2003).
[5]J. Y. Jo, S. M. Yang, T. H. Kim, H. N. Lee, J. G. Yoon, S. Park, Y. Jo, M. H. Jung, and T. W. Noh, Phys. Rev. Lett. **102**, 045701 (2009).
[6]J. Y. Jo, H. S. Han, J. G. Yoon, T. K. Song, S. H. Kim, and T. W. Noh, Phys. Rev. Lett. **99**, 267602 (2007).
[7]W. Li and M. Alexe, Appl. Phys. Lett. **91**, 262903 (2007).
[8]T. Tybell, P. Paruch, T. Giamarchi, and J. M. Triscone, Phys. Rev. Lett. **89**, 097601 (2002).
[9]A. Agronin, M. Molotskii, Y. Rosenwaks, G. Rosenman, B. J. Rodriguez, A. I. Kingon, and A. Gruverman, J. Appl. Phys. **99**, 104102 (2006).
[10]V. R. Aravind, A. N. Morozovska, S. Bhattacharyya, D. Lee, S. Jesse, I. Grinberg, Y. L. Li, S. Choudhury, P. Wu, K. Seal, A. M. Rappe, S. V. Svechnikov, E. A. Eliseev, S. R. Phillpot, L. Q. Chen, V. Gopalan, and S. V. Kalinin, Phys. Rev. B **82**, 024111 (2010).
[11]P. Maksymovych, S. Jesse, M. Huijben, R. Ramesh, A. Morozovska, S. Choudhury, L. Q. Chen, A. P. Baddorf, and S. V. Kalinin, Phys. Rev. Lett. **102**, 017601 (2009).
[12]S. Wicks, V. Anbusathiah, and V. Nagarajan, Nanotechnology **18**, 465502 (2007).
[13]Y. C. Chen, Q. R. Lin, and Y. H. Chu, Appl. Phys. Lett. **94**, 122908 (2009).
[14]Y. C. Chen, G. F. Wang, H. H. Tai, J. W. Chen, Y. C. Huang, J. C. Yang, and Y. H. Chu, Nanotechnology **22**, 254030 (2011).
[15]R. K. Vasudevan, Y. Liu, J. Li, W. I. Liang, A. Kumar, S. Jesse, Y. C. Chen, Y. H. Chu, V. Nagarajan, and S. V. Kalinin, Nano Lett. **11**, 3346 (2011).
[16]R. K. Vasudevan, Y. C. Chen, H. H. Tai, N. Balke, P. Wu, S. Bhattacharya, L. Q. Chen, Y. H. Chu, I. N. Lin, S. V. Kalinin, and V. Nagarajan, ACS Nano **5**, 879 (2011).
[17]Y. Kim, S. Bühlmann, S. Hong, S.-H. Kim, and K. No, Appl. Phys. Lett. **90**, 072907 (2007).
[18]J. Woo, S. Hong, N. Setter, H. Shin, J.-U. Jeon, Y. E. Pak, and K. No, J. Vac. Sci. Technol. B **19**, 818 (2001).
[19]Y. Kim, M. Park, S. Bühlmann, S. Hong, Y. K. Kim, H. Ko, J. Kim, and K. No, J. Appl. Phys. **107**, 054103 (2010).
[20]A. Gruverman and M. Tanaka, J. Appl. Phys. **89**, 1836 (2001).
[21]V. Nagarajan, S. Aggarwal, A. Gruverman, R. Ramesh, and R. Waser, Appl. Phys. Lett. **86**, 262910 (2005).
[22]A. Roelofs, N. A. Pertsev, R. Waser, F. Schlaphof, L. M. Eng, C. Ganpule, V. Nagarajan, and R. Ramesh, Appl. Phys. Lett. **80**, 1424 (2002).
[23]C. S. Ganpule, A. L. Roytburd, V. Nagarajan, B. K. Hill, S. B. Ogale, E. D. Williams, and R. Ramesh, Phys. Rev. B. **65**, 014101 (2001).

[24]V. Anbusathaiah, V. Nagarajan, and S. Aggarwal, J. Appl. Phys. **101**, 084104 (2007).
[25]R. R. Mehta, B. D. Silverman, and J. T. Jacobs, J. Appl. Phys. **44**, 3379 (1973).
[26]C.-H. Yang, J. Seidel, S. Y. Kim, P. B. Rossen, P. Yu, M. Gajek, Y. H. Chu, W. Martin, M. B. Holcomb, Q. He, P. Maksymovych, N. Balke, S. V. Kalinin, A. P. Baddorf, S. R. Basu, M. L. Scullin, and R. Ramesh, Nature Mater. **8**, 485 (2009).
[27]W. Wu, J. R. Guest, Y. Horibe, S. Park, T. Choi, S. W. Cheong, and M. Bode, Phys. Rev. Lett. **104**, 217601 (2010).
[28]P. Maksymovych, S. Jesse, P. Yu, R. Ramesh, A. P. Baddorf, and S. V. Kalinin, Science **324**, 1421 (2009).
[29]V. Garcia, S. Fusil, K. Bouzehouane, S. Enouz-Vedrenne, N. D. Mathur, A. Barthelemy, and M. Bibes, Nature (London) **460**, 81 (2009).
[30]H. Ko, K. Ryu, H. Park, C. Park, D. Jeon, Y. K. Kim, J. Jung, D.-K. Min, Y. Kim, H. N. Lee, Y. Park, H. Shin, and S. Hong, Nano Lett. **11**, 1428 (2011).
[31]J. Kim, Y. Kim, K. No, S. Bühlmann, S. Hong, Y.-W. Nam, and S.-H. Kim, Integr. Ferroelectr. **85**, 25 (2006).
[32]Y. Kim, C. Bae, K. Ryu, H. Ko, Y. K. Kim, S. Hong, and H. Shin, Appl. Phys. Lett. **94**, 032907 (2009).
[33]J. Woo, S. Hong, D. K. Min, H. Shin, and K. No, Appl. Phys. Lett. **80**, 4000 (2002).
[34]Y. H. Chu, M. P. Cruz, C. H. Yang, L. W. Martin, P. L. Yang, J. X. Zhang, K. Lee, P. Yu, L. Q. Chen, and R. Ramesh, Adv. Mater. **19**, 2662 (2007).
[35]J. Wang, J. B. Neaton, H. Zheng, V. Nagarajan, S. B. Ogale, B. Liu, D. Viehland, V. Vaithyanathan, D. G. Schlom, U. V. Waghmare, N. A. Spaldin, K. M. Rabe, M. Wuttig, and R. Ramesh, Science **299**, 1719 (2003).
[36]F. Zavaliche, S. Y. Yang, T. Zhao, Y. H. Chu, M. P. Cruz, C. B. Eom, and R. Ramesh, Phase Transitions **79**, 991 (2006).
[37]R. G. Palmer, D. L. Stein, E. Abrahams, and P. W. Anderson, Phys. Rev. Lett. **53**, 958 (1984).
[38]X. Fang and T. Kobayashi, Appl. Phys. A **69**, S587 (1999).
[39]S. J. Clark and J. Robertson, Appl. Phys. Lett. **90**, 132903 (2007).
[40]S. M. Sze, *Physics of Semiconductor Devices*, 2n ed. (Wiley, New York, 1981).
[41]W. Merz, Phys. Rev. **95**, 690 (1954).